Journal of Marine Systems 189 (2019) 36–49

Contents lists available at ScienceDirect

Journal of Marine Systems

journal homepage: www.elsevier.com/locate/jmarsys

Environmental changes reflected by sedimentary geochemistry for the last one hundred years of a tropical estuary

José Lourenço Friedmann Angeli[a,*], Belén Rubio[b], Bianca Sung Mi Kim[a], Paulo Alves de Lima Ferreira[a], Eduardo Siegle[a], Rubens César Lopes Figueira[a]

[a] Oceanographic Institute, University of São Paulo, 05508-120 São Paulo, Brazil
[b] Marine Geoscience Department, University of Vigo, 36310 Vigo, Pontevedra, Spain

ARTICLE INFO

Keywords:
Geochemistry
Organic matter sources
Estuarine sediments
Caravelas estuary
Brazil

ABSTRACT

Based on multiple proxies, such as major and trace elements, mineralogy, C_{org}/N_{total} ratio and $\delta^{13}C$, we assessed the natural and anthropogenic depositional record in a tropical estuary (Caravelas, Brazil). The Caravelas estuary was once a pristine area of highly important ecological role, due to its mangroves and proximity to the largest reef system in the South Atlantic (Abrolhos Archipelago). However, during the past decades, the estuary has been subjected to both natural and anthropogenic impacts, such as a natural opening of an inlet and changes in land use. This study is based on three dated cores, taken from the inlet to the main channel. A shift in the organic and inorganic proxies, in the early 1960s, shows the impact of this natural opening on the hydrodynamics and sediment distribution. Furthermore, there is a clear spatial pattern in the contribution of the main sources to the organic matter content in the cores: the core collected further away from the inlet shows a strong C3 plant contribution while the ones recovered closer show a higher marine influence. Only a slight increase in enrichment factors of the selected trace metals has been observed and they have been attributed to land use changes rather than direct inputs from industrial and urban sources. Such information is vital for the effective management of coastal systems, mainly when considering natural and ongoing anthropogenic changes in its forcing conditions that are exacerbated by climate change.

1. Introduction

Coastal and estuarine sediments often preserve a continuous record of regional and even global environmental changes, which can be employed in reconstructing environmental evolution and assess anthropogenic impacts (Guo and Yang, 2016) Depending on their source, they incorporate a 'natural lithogenic component' (Schropp and Windom, 1988) and a 'natural biogenic component' (Álvarez-Iglesias and Rubio, 2012). They also include the supplies from human activities, usually referred to as the 'anthropogenic component' which includes both organic and inorganic inputs. These has been especially significant in the last hundred years, where coastal zones have been remarkably modified by urban, industrial and port development, leading to a widespread contamination of the aquatic ecosystem (Di Leonardo et al., 2012; Montero et al., 2013; Álvarez-Vázquez et al., 2017).

During the last several decades, modifications in the environment, such as those related to hydrodynamics and sediment dispersion, origin and fate of organic matter and trace metal contamination, have gained increasing interest worldwide. Therefore, a pool of proxies has been proved as powerful tools to indicate sedimentary environmental alterations. Among them, the elemental composition and grain size distribution can be used as proxies of terrigenous inputs (Mahiques et al., 2009; Gyllencreutz et al., 2010), and/or organic matter composition (Prahl et al., 1994; Mahiques et al., 2009; Souza et al., 2013), as a productivity proxy.

The Caravelas region is one of the earliest urban occupied areas on the NE Brazilian coast. The region is inserted into the Atlantic Forest Biome (Angeli et al., 2016) and has an important ecological role due to its mangroves and its location next to the Abrolhos coral reef, the largest reef system of the Southern Atlantic Ocean and with the largest diversity of coral reefs of Brazil (Spano et al., 2014). Although not considered impacted by industrial activities, the region has been subjected to significant anthropogenic influences, especially in the last 50 years, due to land uses and various economic activities such as wood exploitation, fishing and agricultural activities (Sousa et al., 2014). Leipe et al. (1999) pointed out a severe deforestation in the watershed of southern Bahia, indicating that the forest coverage was 85% in 1945, while it lowered down to 6% in 1990. Moreover, during the past decade

* Corresponding author.
E-mail addresses: louangeli14@gmail.com, louangeli@usp.br (J.L.F. Angeli).

https://doi.org/10.1016/j.jmarsys.2018.09.004
Received 8 November 2017; Received in revised form 14 August 2018; Accepted 14 September 2018
Available online 21 September 2018
0924-7963/ © 2018 Elsevier B.V. All rights reserved.

the outer part of the inlet channel has been subjected to dredging operations. These anthropogenic activities can modify the contribution from different sources of organic matter, can lead to an increase in certain metals in the sedimentary record and affect trace element fluxes.

Previous studies, regarding sedimentation rates and geochemistry, have been performed at the Abrolhos reef (e.g., Dutra et al., 2006; Silva et al., 2013; Souza et al., 2013), however such studies are scarce in the Caravelas region and limited to only one sector of the estuary (Sousa et al., 2014; Angeli et al., 2016). Furthermore, none of these studies quantified the fluxes of trace metals to the system. Despite the importance of the Caravelas estuary in the context of the Abrolhos coral reef little is known about the temporal evolution of some key environmental variables, such as major and trace metals, mineralogy and organic matter composition, that are important for management purposes in this the coastal region.

Thus, we aim to assess the impacts of natural processes and anthropogenic activities during the last hundred years in the Caravelas estuary, following a multidisciplinary approach combining sedimentological, geochemical, mineralogical and chronological data to extract useful information on sedimentary processes, elucidate environmental changes and provide insights of the development of the Caravelas region. These results will be useful as reference values for trace element fluxes in estuarine environments, management of vulnerable estuaries and decision making on anthropogenic chronic chemical hazards.

2. Study area

The Caravelas-Peruipe rivers Estuarine System, is a shallow coastal plain environment, located in in South Bahia State (BA), northeastern Brazilian Coast (Fig. 1). This estuarine system is composed of several meandering channels around the Cassumba Island and consists of two estuaries, the Caravelas river in the north, and the Peruípe river in the south, bordering the cities of Caravelas and Nova Viçosa (Andutta et al., 2013), with approximately 2,0.740 and 44,052 inhabitants (IBGE, 2017), respectively. The interconnection channels between the river mouths are 30 m wide in the narrowest reaches, and nearly midway, there is a wider mudflat area that is considered the nodal point for tidal propagation (Schettini et al., 2013).

The Caravelas estuary contains two inlets: the wider (~900 m) and shallower (~8 m) Barra Velha inlet and the narrower (~350 m) and deeper (~25 m) Tomba inlet (Schettini et al., 2013), which is relatively recent (the late 1950s). This inlet was formed by the erosion of the sand spit, which allowed the formation of an estuarine creek that evolved into a 400 m wide and 25 m deep channel (Sousa et al., 2014). Although the actual volumetric contribution of this inlet is similar to that of the original one (Barra Velha), the tidal flow constriction results in spring tidal currents that exceed $1.5\ m\ s^{-1}$. The high shear there led to a stronger erosion and transport rates, and then it constituted an important connection for the material available at the inner shelf to be transported into the estuary (Schettini et al., 2013). Estuarine dynamic changed after the Tomba inlet opening, according to numerical experiments where pre- and post-opening conditions were compared (Siegle, 2016). After this opening, estuarine water residence time was reduced with more water exchange between the estuary and the nearby ocean. It has also changed the residual flow in the interconnecting channel, which is currently directed toward the Caravelas estuary, a fact also observed by Schettini et al. (2013). The natural opening of the inlet contributed to the modification in sedimentation rates and grain size distribution in the outer sector of the estuary (Angeli et al., 2016). Furthermore, the outer part of the inlet channel has been subjected to dredging operations during the last decade in order to keep a navigation channel open (Sousa et al., 2014).

The Caravelas and Peruípe (Nova Viçosa) rivers are the main rivers of the estuarine system. The first has as main tributaries the Cupido and Jaburuna rivers whose discharges are governed by the precipitation regime in the catchment area of southern Bahia, receiving the water from a small drainage basin ($600\ km^2$) and its river discharge is not monitored. Nonetheless, regional patterns could be estimated at $4\ m^3\ s^{-1}$and $32\ m^3\ s^{-1}$ for the dry and wet seasons (Schettini and Miranda, 2010). Meanwhile, the Peruípe river has a drainage basin of $4600\ km^2$ and its river discharge is monitored daily at the Helvécia station (No. 5510000) by the Brazilian National Agency of Water (*Agência Nacional de Águas – ANA*). This station covers a large part of the drainage basin of the river of approximately $2840\ km^2$ (Andutta et al., 2016), and the mean discharge there is of $20\ m^3\ s^{-1}$ (Schettini and Miranda, 2010). The total annual discharge, according to historical data (1975–2013) from the Brazilian National Agency of Water (ANA, 2016), showed a significant variation, with a maximum average discharge of $40\ m^3\ s^{-1}$ in the early 1990s and minimum averages of approximately $10\ m^3\ s^{-1}$ in the late 1980s and early 2000.

The mean annual rainfall has been recorded as approximately $1570\ mm\ yr^{-1}$ (D'Angiolella et al., 2005). The rainy season is from December to February, and the dry season is from August to September. This region presents a standard atmospheric circulation that varies with the seasonal migration of the anticyclonic cell of the South Atlantic, where NE wind predominate during spring-summer and E-SE winds prevail during autumn-winter (Leão and Dominguez, 2000).

The coral reef system of the Abrolhos Bank is located between 15 and 65 km off the coast. In general, tropical surface waters (TSW) of the southward meandering Brazil Current (BC, $T > 18\ °C$ and $S > 36.0$) overflow the Abrolhos bank and dominate the circulation off the coast (Summerhayes et al., 1976). Suspended particulate matter between the coast and the inner arc of the reef is mainly composed by kaolinite clay and reworked fossil carbonate fragments, resuspended from nearshore shoals (Leipe et al., 1999). Previous studies by Leão et al. (2006) and Silva et al. (2013) about the Abrolhos reefs showed that the continent-derived sediment in the nearshore reef surrounding constitutes up to 70% of the surficial bottom sediment and has two major sources: the reworked sediment from the erosion of hinterland outcrops and the river loads transported to the reef area by alongshore currents.

The mangrove forests of the Caravelas estuary are located close to the Abrolhos reef system (some of the coral reefs are only approximately 15 km offshore), which gives them a great importance for the conservation of their functional and structural attributes. The composition of mangrove species is strongly organized by intertidal and estuarine zonation patterns. *Rhizophora mangle* dominates zones with higher tidal frequency, while *Avicennia schaueriana* dominates zones with a higher saline influence (Soares et al., 2008). Furthermore, according to the work by Souza (2015), where satellite images of the Caravelas Coastal Plain over the years 1984, 1991, 2006 and 2011 were analyzed, the region has been subjected to a gradual expansion of the agricultural area, urban area and pasture, in parallel with the reduction of the areas occupied by water bodies, wetlands and mangroves.

The inner shelf and the estuarine intertidal areas are primarily muddy (Falcão and Ayres Neto, 2010). The lower estuarine channels are composed by fine sands within deeper parts covered by medium to coarse silt. Moving off shore through the inlet sediments becomes coarser being composed by medium to coarse sands (Barroso, 2009).

Although there are no direct measurements of the rivers suspended loads, Schettini and Miranda (2010) found that the concentration of suspended particulate matter (SPM), in the Caravelas main channel, is closely related to the tidal variation and decrease landward from $50\ mg{\cdot}L^{-1}$ at the estuary mouth, to $10\ mg{\cdot}L^{-1}$ at distances of 9 and 16 km for the low and high tide conditions. Furthermore, the total residual SPM transport was out of the estuary at rates of approximately 18 tons per tidal cycle (Schettini and Miranda, 2010).

The estuarine dynamic is primarily driven by tides, the tidal oscillation is classified as meso-tidal and semi-diurnal (Schettini et al., 2013), ranging between 1.5 and 3 m in neap and spring tides, respectively (Teixeira, 2006). The water column presents a vertical structure with well-mixed salinity and pronounced ebb-dominant currents

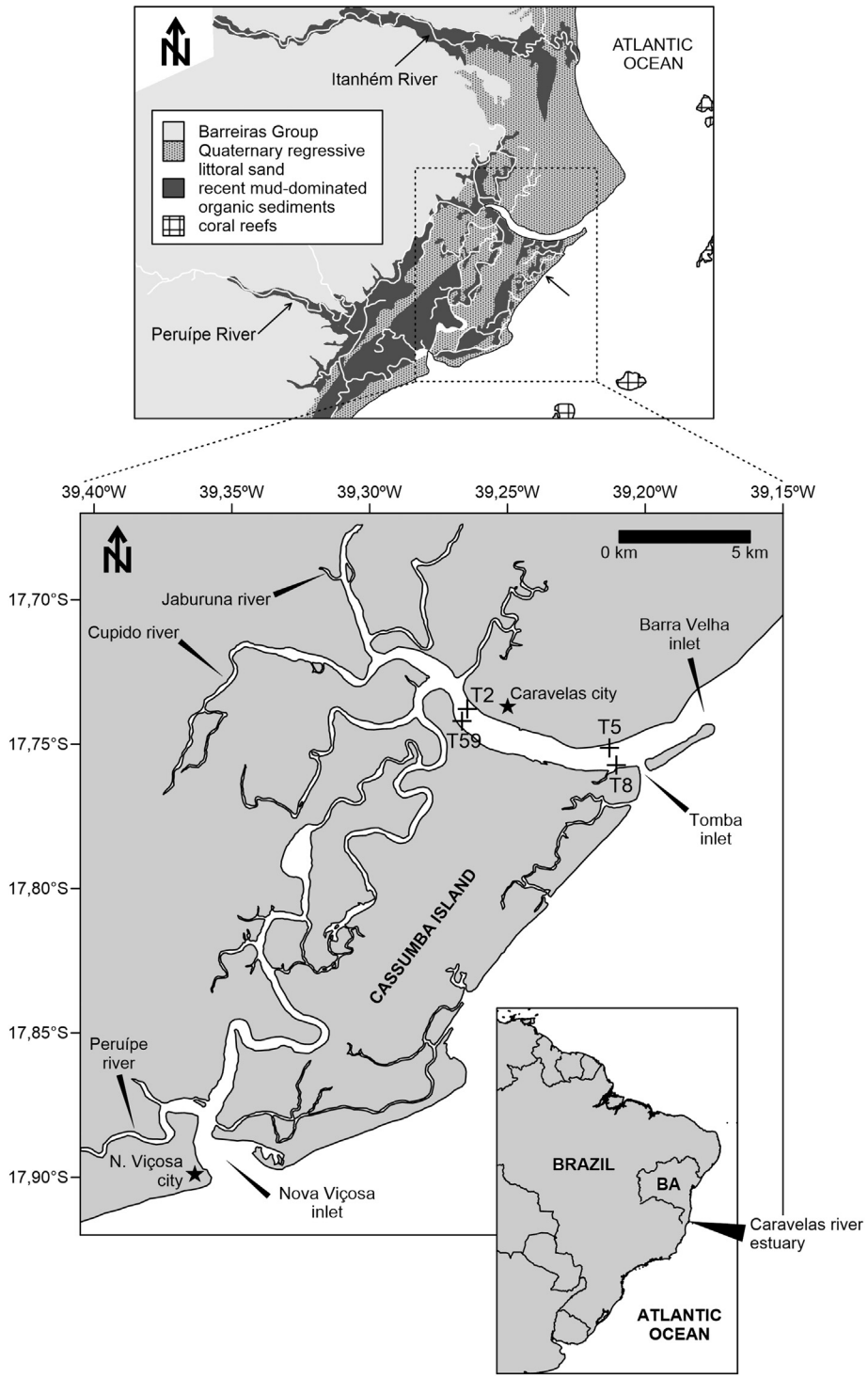

Fig. 1. Location of the Caravelas Estuary in Brazil and detail of the core sampling points: T2, T5 and T8 from this paper. The T59 core location from Sousa et al., 2014 is also plotted.

(Schettini and Miranda, 2010). The transport of suspended particulate matter does not change much between dry and wet periods due to the negligible freshwater inflow compared to the tidal prism (Pereira et al., 2010). Considering the negligible continental inflow, the fined grained sediments that reach the inner part of the estuary could come from the inner shelf rework and transport-up estuary or from the Peruípe river via the interconnection channel with the Nova Viçosa estuary (Schettini et al., 2013).

According to a recent study (Angeli et al., 2016) an increase in the sedimentation rates has been detected since the early 1960s, related to the different processes, both natural (opening of the Tomba inlet) and anthropogenic (land use changes such as wood exploitation, expansion of Eucalyptus culture related to the cellulose industry, construction of a main navigation channel). In addition, a sharp sedimentation rate was detected in the early 2000s related to the beginning of an ebb tidal delta dredging project in front of the Tomba inlet (Lessa and Cirano, 2006).

Based on previous chronologies obtained by ^{210}Pb and ^{137}Cs dating, mean sedimentation rates of 1.22 ± 0.15 cm yr^{-1} (Sousa et al., 2014) and 1.07 ± 0.13 cm yr^{-1} (Angeli et al., 2016) were determined in the middle sector of the estuary (see core position in Fig. 1). Meanwhile, in

the estuary mouth, values of $0.65 \pm 0.06\ cm\ yr^{-1}$ and $0.85 \pm 0.09\ cm\ yr^{-1}$ were determined (Angeli et al., 2016). Therefore, the sector further away from the estuary mouth, characterized by the presence of mangroves and tidal flats (Andrade and Dominguez, 2005), has higher sedimentation rates due to the low currents intensity in this region, demonstrating the influence of the mangrove systems which act as sediment traps (Angeli et al., 2016).

3. Material and methods

3.1. Sampling

The sediment cores T2 (17°44.267′S, 39°15.850′W), T5 (17°45.041′S, 39°13.103′W) and T8 (17°45.446′S, 39°12.600′W) were sampled in August 2013. The recoveries were 232 cm (T2), 144 cm (T5) and 122 cm (T8). All cores were collected using vibracore at the margins of the main channel with maximum depths of 2.5 m. Core T2 was located at the middle sector next to a core sampled by Sousa et al. (2014). This is a sheltered portion of the estuary which is characterized by the presence of mangroves and tidal flats. Meanwhile, cores T5 and T8 were collected in the outer sector of the estuary, where an intense seawater flux landwards dominates, according to Angeli et al. (2016). Core recoveries were 232 cm (T2), 144 cm (T5) and 122 cm (T8).

3.2. General analyses

Each core was longitudinally split and then sliced into 2 cm layers. All samples were frozen until analysis. Once, in the laboratory, bulk samples were lyophilized weighted, and sediment water content was measured (though a gravimetric procedure) by weighing before and after lyophilization.

Grain size analyses (< 63 μm) were conducted in 117 samples for core T2, 50 for core T5 and 59 for core T8 through wet sieving using a 63 μm mesh sieve. This grain size values have been described in Angeli et al. (2016) and will be used for interpreting the obtained results. Calcium carbonate content was determined based in the sample weight difference before and after carbonate removal with concentrated HCl (37%; P.A).

Elemental and stable isotope analyses were performed using an Elemental Analyzer (EA) from Costech coupled with an Isotopic Ratio Mass Spectrometer (IRMS) (Finnigan, model Delta V Plus). Subsamples of sediments for total organic carbon (TOC) and $\delta^{13}C$ analyses were acidified with HCl (1 N) to remove all carbonates. Bulk samples were used for total nitrogen (TN) analysis. The reference standard for $\delta^{13}C$ was the Vienna PeeDee Belemnite (VPDB). Replicate analyses (n = 10) yielded a mean precision of 0.1% for TOC and 0.02% for TN. The analytic precision for $\delta^{13}C$ was 0.1‰. The C/N ratio was calculated considering the ratio between TOC and TN and it will be referred to as C/N throughout the text.

Major element content (Si, K, Na, Ca, Mg, Fe, Sr and Mn) was determined by X-Ray Fluorescence (XRF) analysis in a Siemens SRS 3000 spectrometer. This analysis was carried in 31 samples for core T2, 35 for core T5 and 28 for core T8. Accuracy and precision in major element determinations were verified by analyzing the certified reference material PACS-2 (NRCC, Canada). Results indicated a good agreement between certified and analytical values (recovery was > 82% for the studied elements).

Mineralogy was determined by X-Ray Diffraction (XRD) analysis in a Siemens D-5000 X-ray diffractometer using Cu Kα radiation with unoriented samples. This analysis was performed on the same samples as those of XRF. Scans were run between 2° and 70° 2θ. The abundance of minerals was interpreted from the size of the strongest diffraction peak for each mineral on the X-ray trace of the unoriented powder. The semi-quantitative phase analysis was performed with the software PANalytical X'Pert Highscore plus. A JEOL JSM-6700F microscope was used to observe pyrite morphologies and sizes by Scanning Electron Microscopy (SEM) on selected samples T5 (10 cm) and T8 (60 cm), and for this purpose, samples were placed in aluminium holders and coated with carbon. XRF, XRD and SEM analyses were performed in a specialized laboratory (C.A.C.T.I., Universidad de Vigo, Spain).

A partial digestion technique was performed in 117 samples for core T2, 50 for core T5 and 59 for core T8, according to the method of the US EPA 3050B (USEPA, 1996). Briefly, about 1.0 g of dried sediment aliquot was taken in a 50 ml beaker and then 5 ml of HNO_3, 2.5 ml of H_2O_2 (30% V/V), and 5 ml of HCl were added. Digestion was performed at 90 °C. Subsequently, all treated samples were filtered and diluted to 50 ml with ultrapure water (Milli-Q). It is important to mention that this method involves a strong acid digestion that dissolves the "environmentally available" elements, excluding only those bound to the silicate structures that are not typically mobile in the environment, then element concentrations will be "pseudo-total". The elements Al, As, Cr, Cu, Fe, Ni, Pb, Sc and Zn were measured using Inductively Coupled Plasma Optical Spectrometry (ICP-OES).

The quality control was made considering precision, recovery and Method Detection Limit (MDL) and Method Quantification Limit (MQL). A certified Reference Material (CRM) SS-2 EnviroMAT Contaminated Soil from SCP Science (140-025-002) and blanks were submitted to the same analytical procedure and the results are given in Table 1. Once the confidence interval was within the certified value, the relative standard deviation below 20% and recovery values within 75–125% as recommended by USEPA (1996), it was possible to validate the method since it presented accuracy and precision.

3.3. Mass accumulation rates

Mass accumulation rates (MAR) were calculated based on the excess ^{210}Pb ($^{210}Pbxs$) activity profiles obtained for the studied cores by Angeli et al. (2016).

The mass accumulation rates can be shown to be given directly by the formula:

$$MAR = \frac{kA}{C}$$

where, k is the constant decay for ^{210}Pb ($0{,}0311\ yr^{-1}$); C is the excess ^{210}Pb activity in a given layer and; A is the cumulative residual excess ^{210}Pb (Appleby and Olfield, 1978; Lubis, 2006).

Table 1
Analyzed MDL, MQL, confidence interval, relative standard deviation and recovery of Certified Reference Material.

Element	MDL ($mg\ kg^{-1}$)	MQL ($mg\ kg^{-1}$)	Confidence interval ($mg\ kg^{-1}$)	Mean ($mg\ kg^{-1}$)	% RSD	Recovery (%)
Al	0.28	1.40	12,1114–14,416	13,479	8	102
As	0.19	0.40	65–85	76.4	7	101
Cr	0.09	0.45	30–38	32.5	3	95
Cu	0.14	0.42	182–200	188.9	3	98
Fe	0.06	0.33	19,597-22,495	22,422	12	107
Ni	0.18	0.89	50–58	54.4	2	100
Pb	0.29	0.89	116–136	132.1	5	105
Zn	0.29	1.44	444–490	467.4	4	100

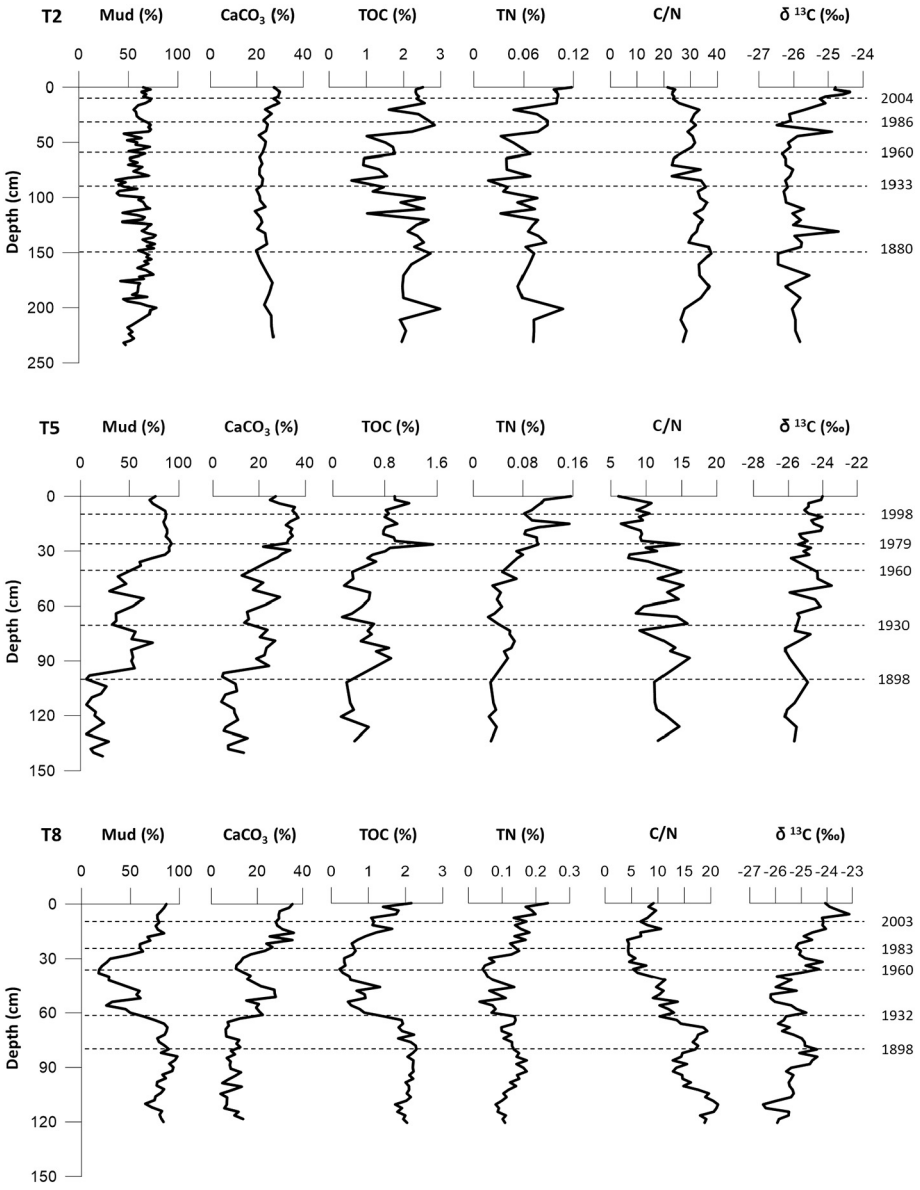

Fig. 2. Vertical distribution of mud content from Angeli et al. (2016), $CaCO_3$, TOC, TN, C/N and $\delta^{13}C$ along the sediment cores from the Caravelas estuary. The equivalence age-depth at some levels has been indicated through dashed lines.

3.4. Element fluxes

Based on the elemental analysis results, element fluxes were calculated by multiplying the element concentrations by the mass accumulation rate (derived from the ^{210}Pb dating method) according to Cochran et al. (1998) with the formula:

$$Fi = Si\ [Me]$$

where Fi = metal flux at i interval (mg cm^{-2} yr^{-1}), Si = the accumulation rate derived from ^{210}Pb method (g cm^{-2} yr^{-1}) and Me = metal concentration (mg g^{-1}) at i interval.

4. Results

4.1. Sediment characteristics

The inner sediment core T2 consisted predominantly of fine-grained sediments (< 63 μm) which showed a relatively stable profile (61.4% ± 9.9%; Fig. 2) except during the 1940–1980 periods where their content oscillates around 45–65%. It is observed a decrease in the fine-grained content, then, an increase until 2004, which maintains afterwards upwards. Contents of calcium carbonate in T2 varied between 19.22 and 29.78%, meanwhile in cores T5 and T8 it is observed an increase from approximately 20% to 30% in the early 1960s (Fig. 2).

The sediment cores located next to the estuary mouth (T5 and T8) showed a stronger variation in grain size (Fig. 2) in their depth profile when compared to the core located in the middle estuary (T2). The sediment core T5, placed near the Barra Velha inlet, showed a significant variation in particle size distributions in the vertical profile, with a predominance of coarse particles (sand) at the bottom of the core. An increase in the average values of the fine-grained particles content (from 15.14% to 48.84%) is observed at 100 cm depth (estimated date: 1898 ± 14). A further increase (48.84% to 82.17%) is observed in the early 1960s. This is also the case for sediment core T8, where a significant increase in the fine-grained particles content occurred during the same period (estimated date: 1962 ± 6). In all studied cores the presence of gravels was not observed.386.

Based on the XRD analyses, sediments from T2 core displayed a relatively homogeneous mineralogy, except for pyrite. The primary

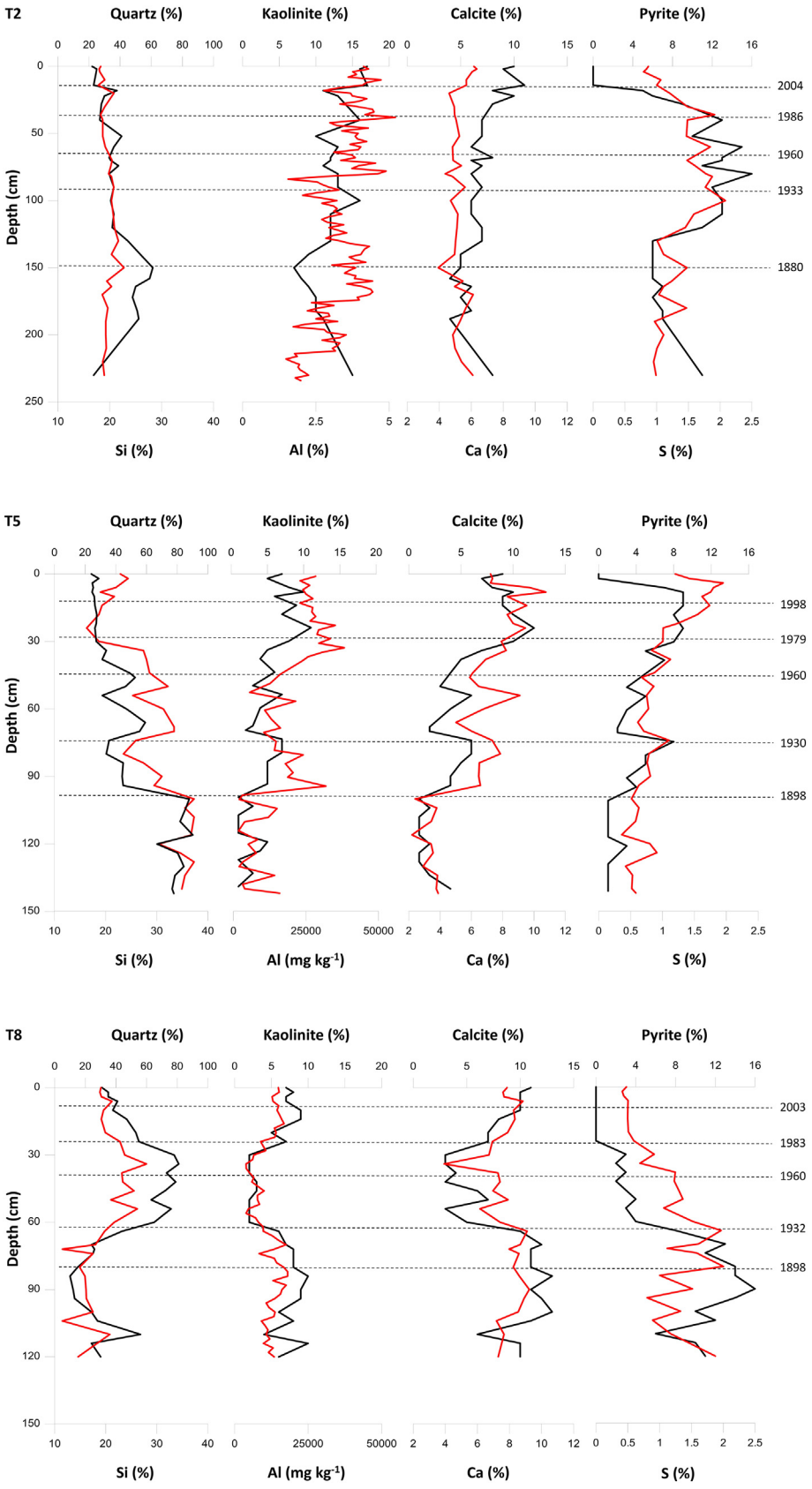

Fig. 3. Vertical distribution of the main mineralogical constituents (black) together with the main elements forming these minerals (red), in the studied cores. Al was analyzed trough ICP-OES while Si, Ca and S trough XRF. The equivalence age-depth at some levels has been indicated through dashed lines. (For interpretation of the references to color in this figure legend, the reader is referred to the web version of this article.)

mineralogical constituents found in the sediments were: Quartz, Aragonite, Kaolinite, Calcite and Pyrite (Fig. 3). The mineral content in core T2 ranged 20–60% for quartz, 9–19% for aragonite, 5–17% for kaolinite, 5–11% for calcite and 0–16% for pyrite.

The mineralogy of the T5 and T8 cores was also dominated by the following mineral constituents: Quartz, Aragonite, Calcite and Kaolinite (Fig. 3). In sediment core T5, mineral content ranged 21–91% for quartz, 1–22% for aragonite, 1–11% for kaolinite, 1–12% for calcite and 0–9% for pyrite; whereas for core T8 the mineral content ranged 10–81% for quartz, 9–18% for aragonite, 2–10% for kaolinite, 3–13% for calcite and 0–16% for pyrite.

Depth profiles of Quartz and Si contents were very similar to the depth profiles of sand content. Meanwhile the layers with a high content of fine-grained particles (T5, 10–20 cm; T8, 2–14 cm and 70–100 cm) were characterized by greater amounts of Kaolinite. The presence of the mineral kaolinite points toward the occurrence of chemical weathering of rocks (Rao et al., 2015). The higher quantities of this mineral in the T2 core in front of those situated at the mouth of the estuary (T5 and T8) are related to a higher continental influence, meanwhile the higher contents of Calcite and Aragonite found in the top layers of sediment cores T5 and T8 (up to 30% together) could be explained by the influence of the adjacent shelf rich in carbonates and the presence of the Abrolhos Bank.

Pyrite maxima values are detected in T2 core at intermediate depths (40–120 cm), in T5 core, subsurficially (10–30 cm), and in T8 core at the bottom (70–100 cm). This mineral was present in all sediment cores at certain depths, due to diagenetic processes and its presence was confirmed by SEM analyses of the selected samples from cores T5 and T8. No other sulphides were detected by SEM in the selected samples. Fig. 4 show an abundant amount of pyrite displaying framboidal morphologies. The average size of the framboids in the sediment cores is 10 μm. They are slightly more abundant in the lower parts of the cores, where single euhedral crystals are also observed.

4.2. TOC, TN, C/N and δ13C

In general, the sediment core (T2) showed less variation in the studied proxies, over time, compared to the other two cores that are located next to the estuary mouth (T5 and T8). The sediment core T2 is located in a more protected zone surrounded by mangroves, while the other two are closer to the Barra Velha and Tomba inlets, respectively.

The sediments of T2 showed a relatively high average TOC content of 2.0 ± 0.6% compared to the sediments T5 (0.6 ± 0.3%) and T8 (1.5 ± 0.7%). Between the decades of 1930 and 1960, the TOC values are relatively lower (from 0.6% to 1.8%. An increase of TOC (from 1.0% to 2.2%) is observed for the following more recent periods, in accordance with the values determined by Sousa et al. (2014), in a nearby core (T59). The TN values showed the same trend as TOC (Fig. 2). The $\delta^{13}C$ levels ranged from −26.50 to −24.39‰ indicating, mainly, a C_3 plant contribution to the organic matter.

The TOC and TN contents in the two outer cores showed a higher variability range (Fig. 2), ranging from 0.1 to 1.5% and 0.01 to 0.14% respectively for the sediment core T5 and from 0.2 to 2.3% and 0.03 to 0.24% respectively for the sediment core T8. In sediment core T5 the highest values were detected below surface in the horizon of 1979; whereas in sediment core T8 TOC values were higher in those sediments deposited before 1930. Regarding TN contents in core T5 maximum values were observed at surface and about 15 cm, whereas in T8, at the surface. Furthermore, these sediment cores showed on average higher contents of $CaCO_3$ (up to 35.4‰), lower C/N ratios (from 4 to 20) and higher values of $\delta^{13}C$ (−27 to −23‰) than core T2.

4.3. Trace elements in the sediment cores

The depth profiles of trace elements are presented in Fig. 5. The distribution of As, Cr, Cu, Ni, Pb and Zn, shows, in general, a similar distribution pattern for each core with higher concentrations in levels with a higher content in fine-grained sediments.

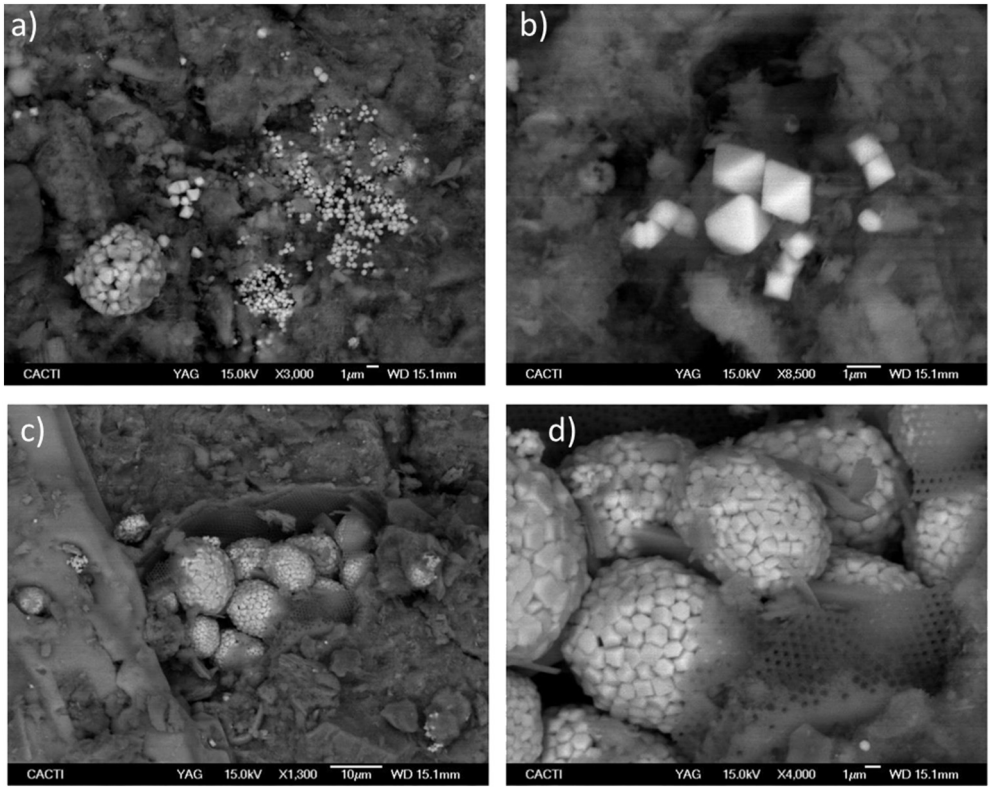
a)
CACTI YAG 15.0kV X3,000 1μm WD 15.1mm
b)
CACTI YAG 15.0kV X8,500 1μm WD 15.1mm
c)
CACTI YAG 15.0kV X1,300 10μm WD 15.1mm
d)
CACTI YAG 15.0kV X4,000 1μm WD 15.1mm

Fig. 4. SEM images for selected samples from the sediment cores from Caravelas estuary. a) Presence of framboidal pyrites and single crystals at a depth of 10 cm in sediment core T5; b) detail of the single crystals (T5; 10 cm); c) cluster of framboidal pyrites (T8; 60 cm); d) detail of a cluster of framboidal pyrites (T8; 60 cm).

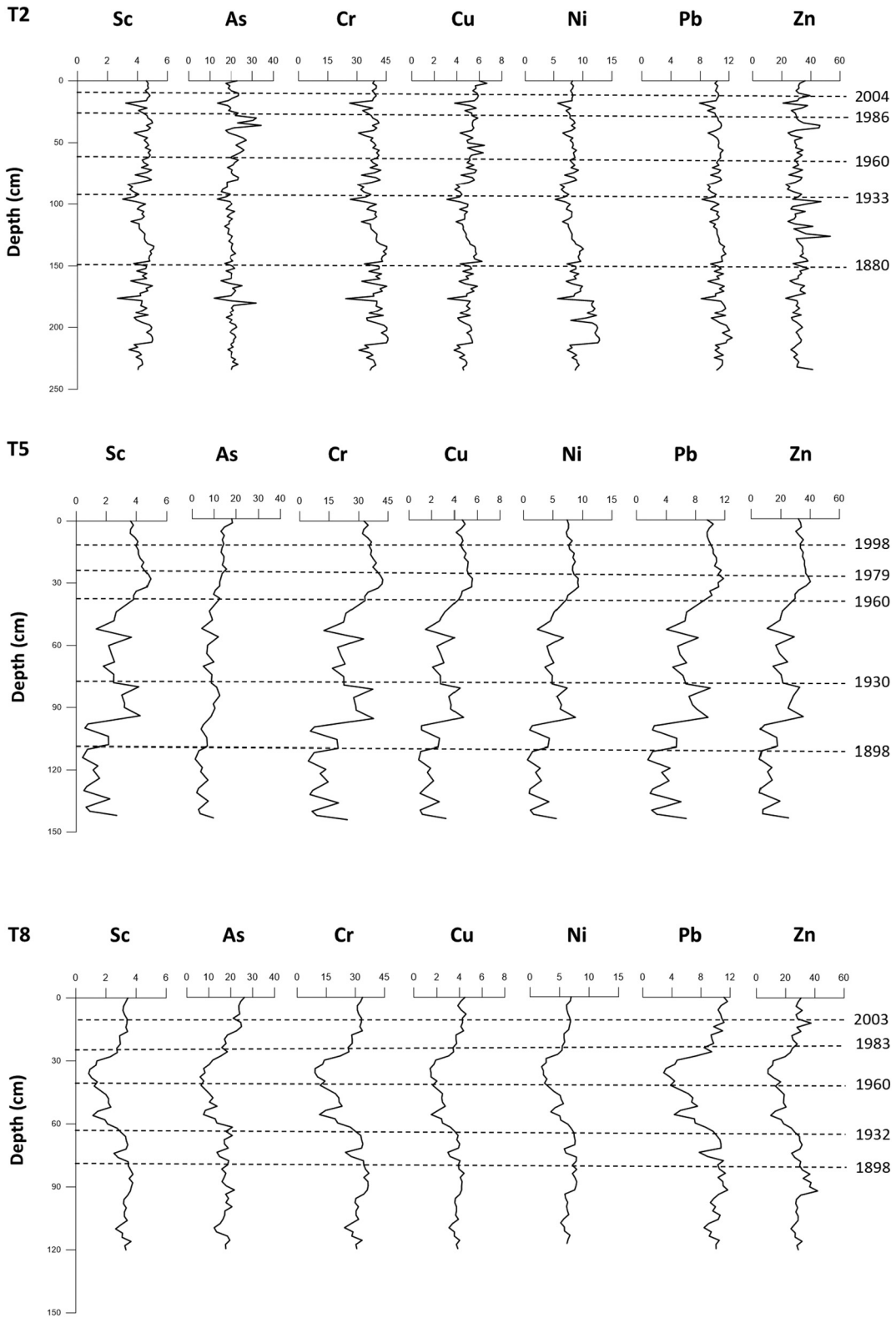

Fig. 5. Vertical distribution of trace elements along the sediment cores from the Caravelas estuary. The equivalence age-depth at some levels has been indicated through dashed lines.

4.4. Mass accumulation rates

The CRS model was applied until depth 110 cm for T2, until 38 cm for T5 and until 50 cm for T8. The evolution of MARs for all sediment cores of interest is presented in Fig. 6. The mass accumulation rates varied from 0.04 ± 0.005 to 1.59 ± 0.19 $g\,cm^{-2}\,yr^{-1}$ in sediment core T2; from 0.02 ± 0.002 to 1.37 ± 0.12 $g\,cm^{-2}\,yr^{-1}$ in sediment core T5 and from 0.39 ± 0.04 to 1.53 ± 0.16 $g\,cm^{-2}\,yr^{-1}$ in sediment core T8. In sediment core T2 there is an upward trend in MARs reaching up 1.6 $g\,cm^{-2}\,yr^{-1}$ in the early 2000s. Sediment core T5

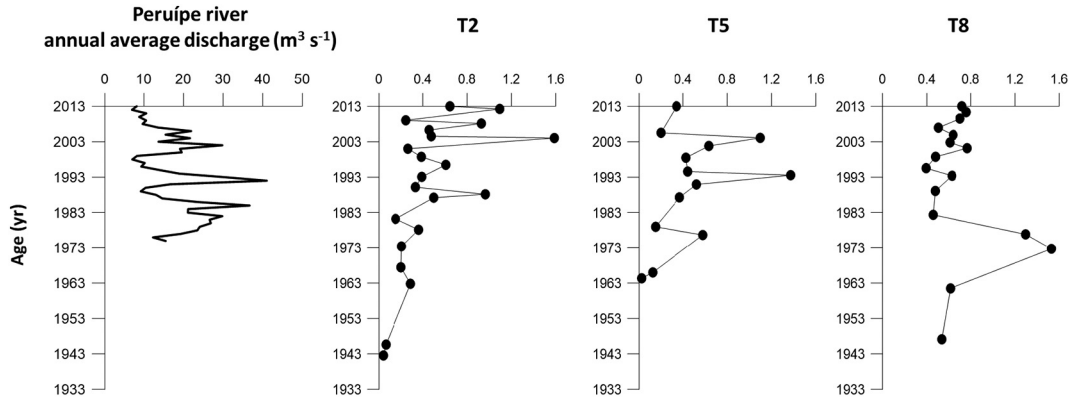

Fig. 6. Annual average discharge of the Peruípe river ($m^3 s^{-1}$) at the Helvécia station between the years 1975 and 2013 (ANA, 2016) and mass accumulation rates (MAR; $g\,cm^{-2}\,yr^{-1}$) vs dating of sediment cores T2, T5 and T8 from the Caravelas estuary.

displays a variable MAR profile with peaks of 1.37 $g\,cm^{-2}\,yr^{-1}$ and 1.10 $g\,cm^{-2}\,yr^{-1}$ in the early 1990s and early 2000s. Finally, in sediment core T8, a peak of 1.53 $g\,cm^{-2}\,yr^{-1}$ in the early 1970s is observed, followed by a decrease to 0.46 $g\,cm^{-2}\,yr^{-1}$ in the early 1980s and then, a general increase until the top layers.

4.5. Fluxes of trace elements to the Caravelas estuary sediments

Element fluxes were calculated according to Cochran et al. (1998) to better understand the accumulation and depletion of elements over time (Fig. 7). Fluxes were only calculated for those layers dated by the CRS model (until 110 cm depth for T2, 38 cm for T5 and 50 cm for T8) covering periods from the early 1940s for core T2, the early 1960s for T5, and around 1950 for T8, to the present. In T2, the fluxes of As, Cr, Cu, Ni Pb And Zn had a general tendency to increase from the early 1970s to the present, displaying a peak maximum in the early 2000s. The fluxes in T5 showed marked increases in the early 1970s, early 1990s and early 2000s. In sediment core T8, there is a general tendency of increase form the early 1960s to the present with a peak maximum in the late 1990s.

5. Discussion

5.1. Sources and diagenesis of organic matter in the Caravelas estuary sediments

All cores presented a significant positive correlation between TOC and mud contents (Core T2, $r^2 = 0.65$; Core T5, $r^2 = 0{,}70$; Core T8, $r^2 = 0{,}74$; $p < 0.05$), as expected and as demonstrated by numerous authors (Helali et al., 2016; Prajith et al., 2016). However, the slightly lower correlation found in the inner core (T2), indicates that in some regions of the Caravelas Estuary organic matter distribution is influenced not only by hydrodynamic conditions and the concurrent sediment depositional patterns, but also by additional factors such as proximity of the source (e.g. mangroves), which may be responsible for local changes in organic matter deposition. Organic material in coastal environments is usually associated with fine-grained sediments (Ogrinc et al., 2005), but this association occurs to a lesser extent in T2 sediments ($r^2 = 0.65$; $p < 0.05$), in which the organic material derived from mangroves may be the primary contributor to the T2 TOC.

The C/N ratio in core T2 showed values (21.38–37.67; Fig. 2) characteristic of terrestrial vegetation contributions (> 12) (Meyers, 1994) since the composition of these higher plants consist predominantly of lignin and cellulose, which contain few nitrogen compounds (Sampei and Matsumoto, 2001; Lamb et al., 2006). The $\delta^{13}C$ values for sediment core T2 (−26.50‰ to −24.39‰) also suggest a terrestrial contribution that may be associated with organic material

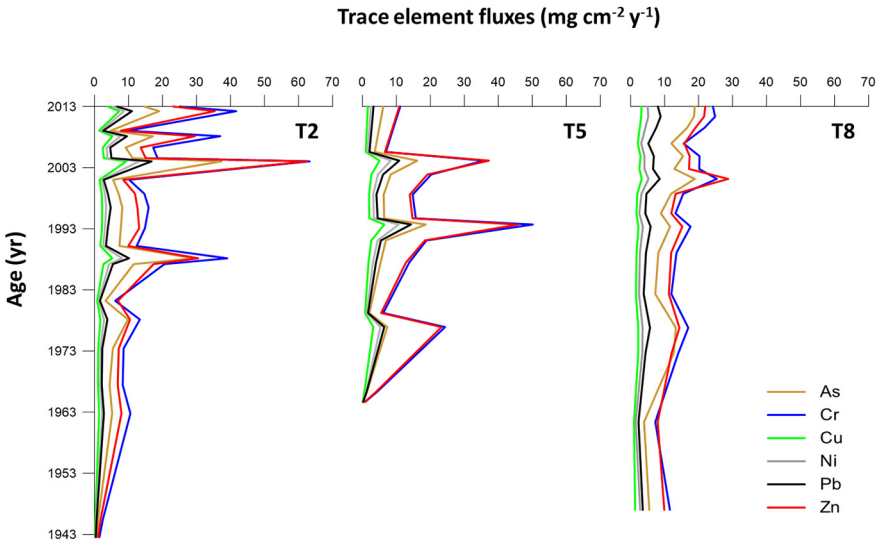

Fig. 7. Trace element fluxes ($mg\,cm^{-2}\,yr^{-1}$) along the sediment cores T2, T5 and T8 of the Caravelas estuary.

from the mangrove forests and from the eucalyptus monoculture (Meyers, 1994, 2003). Values of $\delta^{13}C$ between −29,1‰ to −25‰ were found in red mangrove (*Rhizophora mangle*) leaves (Smallwood et al., 2003), an abundant species in the Caravelas estuary (Soares et al., 2008), meanwhile levels between −25.22 and −29.66‰ were found in eucalyptus leaves (Olbrich et al., 1993), which are typical for C_3 plants.

Direct measurements of currents and suspended sediment concentration performed in the Caravelas Estuary suggested that the inlets and the adjacent inner shelf area are primary sources of suspended sediments. This fine-grained material advects up estuary with a maximum transport at spring tides and null transport at neap tides (Schettini et al., 2013). Furthermore, the Caravelas Estuary still contains mangrove forests that act as trapping areas for fine sediments, as mangrove areas are considered depositional environments (Victor et al., 2004). Possibly, the advection of suspended sediments and associated organic matter from the inlets and the adjacent shelf would have greater influence in the outer estuary, while depositional processes related to mangrove areas should predominate in the inner estuary, where mangrove forests are better preserved.

The C/N ratios and $\delta^{13}C$ isotopic signals suggest a different source of the organic matter between basal and near-surface Caravelas estuary sediments: a predominantly natural terrestrial input was recorded by sediments older than the early 1960s in contrast to the more recent sediments (1960–2013), which instead, record a marine signal. Souza et al., (2013) found mean values of $\delta^{13}C$ of −26.9‰ in mangroves, −20.7‰ in the Caravelas channel region and −18.2‰ in reefs and they associated the observed variation with the main source of organic matter, which for the mangrove is derived from vascular plants (mainly C3 metabolism) while for the reefs come from phytoplankton. Dittmar et al. (2006) indicated that mangroves are the main source of terrigenous DOC to the open ocean off Brazil. In their calculations they considered a $\delta^{13}C$ value of −31.4‰ for DOC from the mangrove end-member and of −23.7‰ for the marine end-member.

The increase in $\delta^{13}C$ values and the decrease in the C/N ratio, since the decade of 1960 show a higher marine influence, possibly due to the opening of the Tomba inlet, which facilitated the transport of sediment up-estuary from the inner shelf. This inlet was opened in the late 1950s and gradually became wider and more effective in exchanging material between the inner shelf and the estuary (Sousa et al., 2014). The newly formed channel gradually became the main channel, through widening and deepening. The initially narrow inlet started widening at a rate of approximately 9 m yr^{-1}, presenting a width of approximately 110 m in 1975 and reaching its present width of approximately 400 m in 2011 (Siegle, 2016). Meanwhile, flow velocity diminished in barra Velha channel (an average reduction of 0.1 m s^{-1} according to Siegle (2016), which became shallower (depths reducing from approximately 7 to 3 m)) during the last decades. This results in particle deposition in the Barra Velha portion.

This higher marine influence after the inlet opening was also detected when studying the foraminifera diversity and density in a core collected close to the core T2 (Sousa et al., 2014; Fig. 1), where an increase in open dweller foraminifera species (*Cassidulina crassa*, *Cornuspira involvens* and *Gavelinopsis praegeri*) was related to inward transport of suspended particles by tidal currents (Sousa et al., 2014). This oceanic influence has been also detected in the Barra Velha mouth (Spano et al., 2014; Sousa et al., 2016). Additionally, according to Debenay et al. (2001), the presence of *Parotalia cananeiaensis* in the estuaries of southern Brazil indicates a landward transport of suspended material via tidal currents in these environments. The increasing contribution of marine sources (dissolved and/or particulate) in all cores after the Tomba inlet opening is identified in the diagram of the C/N ratio versus $\delta^{13}C$ (Fig. 8).

The presence of pyrite in the studied sediments would be probably related to the presence of labile organic matter and to changes in the prevalence of the different organic matter sources. Regarding its

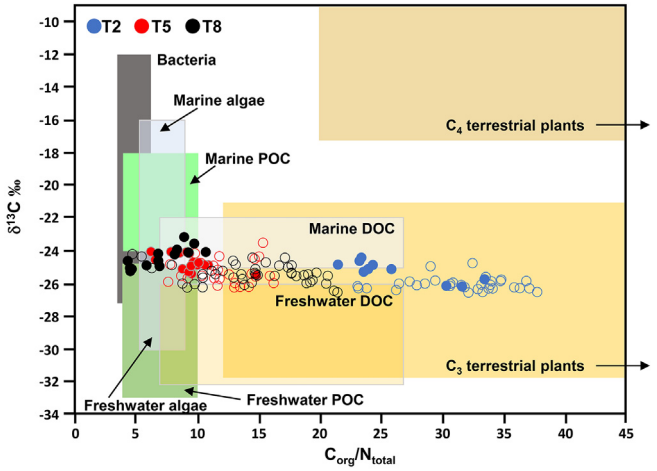

Fig. 8. Plot with $\delta^{13}C$ vs C/N for sediment cores T2, T5 and T8. Adapted from Lamb et al. (2006). Samples are divided as follows: sediments deposited before 1960 (empty circles) and after 1960 (full circles).

contents, those sediment cores located next to the estuary mouth showed a different behavior among them. Sediment core T8 is located in an area next to the Tomba inlet, where the deep currents and turbulence became more intense after its opening and widening (Siegle, 2016). These phenomena favor the remobilization of the sediments, avoiding the establishment of totally anoxic conditions in the superficial layers. On the other hand, with the opening of the Tomba inlet, the Barra Velha inlet, where sediment core T5 is located, underwent a decrease in the intensity of the bottom currents, favoring the settling of fine-grained sediments, and these, together with organic matter promoted the establishment of anoxic conditions, and then, the formation of pyrite.

5.2. *Trace elements in the Caravelas estuary sediments: inputs, sources and assessment of contamination*

Most metals were well correlated among them ($p < 0.05$). The noticeable positive correlations in all sediment cores for Sc vs fine-grained content ($r^2 = 0.60$; $r^2 = 0.91$; $r^2 = 0.94$ for cores T2, T5 and T8, respectively), Sc vs Cr ($r^2 = 0.84$; $r^2 = 0.99$; $r^2 = 0.99$ for cores T2, T5 and T8, respectively), Sc vs Cu ($r^2 = 0.78$; $r^2 = 0.98$; $r^2 = 0.95$ for cores T2, T5 and T8, respectively) and Sc vs Pb ($r^2 = 0.66$; $r^2 = 0.98$; $r^2 = 0.97$ for cores T2, T5 and T8, respectively) confirms that these elements are associated with the fine-grained fraction of the sediment.

Furthermore, Sc and some other metals (Cr, Cu, Pb and Zn) showed depth profiles that parallel the TOC profile, reflecting the association of these metals with organic matter. The sedimentary organic matter may also influence metal concentrations in sediments, suggesting that the accumulation of trace metals is closely related to the accumulation of organic matter. Also, it reflects a similar provenance or post-depositional behavior for such elements. This correlation between the metal concentration and the organic matter content in sediments has been previously shown by various authors (Dai et al., 2007; Ip et al., 2007; Martins et al., 2012).

It is well established that grain-size distribution and organic matter contents are important controlling factors of the abundance of trace metals. Fine-grained sediments tend to have relatively higher metal contents due in part to the high specific surface area of the smaller particles. This enrichment is mainly due to surface adsorption and ionic attraction (Horowitz and Elrick, 1987; Rubio et al., 2000). Also, coatings of organic matter are prevalent in fine-grained sediments, and these coatings bind a variety of trace elements (Wangersky, 1986).

The degree of contamination cannot be established adequately without accounting for textural effects caused by the grain-size

variation of the samples. This is achieved by normalizing the data with a conservative element. Normally, geochemical procedures are performed using conservative elements such as Sc, Al, Fe, V and Li to reduce the natural effects of grain size (Wang et al., 2015). The chosen constituent should be a particle size proxy, lithogenic, conservative, and its concentration should not be anthropogenically altered, meaning that their ratios should remain relatively constant in the crust (Elkady et al., 2015; Wang et al., 2015).

We have chosen to normalize metal concentrations using Sc as a grain-size proxy because it has the best correlation and significative ($p < 0.05$) with the fine-grained sediment in all cores ($r = 0.78$; $r = 0.95$, $r = 0.97$ for cores T2, T5 and T8, respectively). The enrichment factors (EFs) were calculated as follows:

$$EF = \frac{{}^{Me}/_{X}\ sample}{{}^{Me}/_{X}\ Background}$$

where Me is the level of the studied trace element and X is the level of Sc. Background levels (BL) were established by using the average trace element concentrations in the deepest core samples. These samples, considering the chronology (Angeli et al., 2016) represent the pre-anthropogenic conditions.

Enrichment factors depend on the background data used. For the total metal content of the sediments, these data can be provided by the average metal concentration of texturally and mineralogically equivalent sediments, either reported in the literature or measured by the authors in a known pristine region (Loring and Rantala, 1992). The world average shale and the world average soil are among the materials often used to provide background levels. However, these metal levels tend to be very general and may mislead in a specific coastal area (Birch, 2017). This latest author recommends the use of regional background values. Thus, we propose the following BL for the studied area (Table 2).

Metal concentrations in studied sediments are typically not elevated over the BLs. In general, no enrichment was observed with EF values around 1 (Fig. 9). Nevertheless, the EF for arsenic shows slightly elevated values for all cores, presenting moderate enrichment as Álvarez-Iglesias and Rubio (2012) classified (1.56, 1.36, 1.83 for cores T2, T5 and T8, respectively), in the last 40 years, probably related to urban development and industrial wastes, especially from cellulose treatment. Currently, the most widely used wood preservative for timbers exposed in aquatic environment is chromated copper arsenate (CCA) (Hingston et al., 2001). These chemicals leaching form treated wood can be adsorbed onto sediments and be taken up by benthos. A significant portion of these chemicals leaching from wood in an estuary would be expected to be adsorbed onto nearby sediment particles (Weis and Weis, 1993).

The degree of chemical contamination was also assessed considering sediment quality guidelines (Long et al., 1995). According to these authors the concentrations below the Effect range-low (ERL) value represent a minimal-effects range; a range intended to estimate conditions in which effects would be rarely observed. In contrast, Effects range-median (ERM) represent chemical concentrations above which effects are more frequently expected (Long et al., 1995).

Concerning the elemental geochemical data, Cr, Cu, Ni, Pb and Zn concentrations were below their corresponding ERLs, indicating no significant contamination by these elements in the study area (Table 3). Similar trace elements content were found by Sousa et al. (2014, 2016) in sediments collected in the study area. The only element that showed concentrations above the ERL was arsenic although ERM values were not exceeded. Given the absence of significant anthropogenic As sources in this region, the local continental geological formations of the "Barreiras Group" are presumed to be the original source of arsenic. Thus, regarding the inorganic contamination assessed by calculation of enrichment factors and comparison with values of ERL and ERM, the Caravelas estuary can be considered a pristine environment (Table 3).

Furthermore, the elements determined in this study were compared with those of the Barreiras Group, described as the major geological compartment in the region, and composed of Neogene terrigenous sediments (Carvalho et al., 2013) being of the same order for all elements of interest. These sediments have widespread occurrence along the Brazilian coast, extending along the coastal zone from the northern region, as far as the State of Rio de Janeiro and consist dominantly of fine to coarse quartz sands; gray-reddish, purple and yellowish clays and coarse to conglomeratic sandstones, with kaolinite matrix, and commonly impregnated by iron hydroxides deposits (Vilas Boas et al., 2001). These ferruginous sandstones contain significant amounts of As (12.8–23.0 mg kg^{-1}), and their iron hydroxides contain up to 300 mg kg^{-1} of As (Mirlean et al., 2011).

The values of trace elements and the main mineral phases found in this study can be taken as an indicative of the role of the Barreiras Group as an important source of terrigenous materials to the Caravelas estuary.

5.3. MARs and fluxes of trace elements

It is noteworthy that all trace element fluxes (Fig. 7) showed a similar behavior within each sediment core. This could be representative of a main lithogenic source and, the association between them is explained by the ability of fine-grained sediment to scavenge metals. Moreover, in general, despite the peaks displacement related to the standard deviation of the chronology data, all sediment cores showed marked increases in trace element fluxes corresponding to maximum average discharges of the Peruípe river through the interconnecting channel, confirming the significant role of this river in the sediment supply to the Caravelas estuary.

It seems that MARs conditioned the trace element fluxes for T2 and T5 cores, while for core T8 the marked peak in MARs at 1973–1980 results in a small maxima in trace metal fluxes, while the highest fluxes are detected around mid-1990s. This marked peak in MARs at 1973–1980 in core T8 could be related to a higher influx of sand to this core, and, consequently, less metal adsorbed.

The peak in trace element fluxes in core T2 and T5 in 2005 are coincident, happening after a peak in the river discharge. The peak in river discharge in 1993 has its reflection in the flux a few years after in T5 core profiles (also less marked in T8). The peak in flux before 2003 is reflected by a peak in T8 core. The discharge peak in 1985 is reflected by a peak in T2 at about 1990. There is a less marked peak in T5 and T8 cores at about 1980. The difference between the flux tendencies of the sediment cores may result from the sedimentary processes occurring at each site. These differences could be attributed to the location of each sediment core, with sediment core T5, located closer to the interconnection channel, showing more influence of the Peruípe river flows.

The effects of the interconnecting channel and its influence on trace element inputs can be clearly observed in the temporal profiles of the

Table 2
Background levels (BL) for trace elements for the Caravelas estuary sediments (this study) established considering the deepest core samples concentrations, compared to global references.

BL (mg kg^{-1})	As	Cr	Cu	Ni	Pb	Zn	Reference
Global[a]	13	90	45	68	20	95	Turekian and Wedepohl (1961)
Global[b]	13	90	250	225	80	95	Turekian and Wedepohl (1961)
Global[c]		90		68		95	Wedepohl (1971, 1991)
T2	21.08	37.78	4.65	8.86	10.80	31.87	This study
T5	5.12	12.93	1.82	2.72	3.89	13.05	This study
T8	17.40	30.26	3.73	6.22	9.83	28.11	This study

[a] Shales.
[b] Deep-sea sediments.
[c] Average shale.

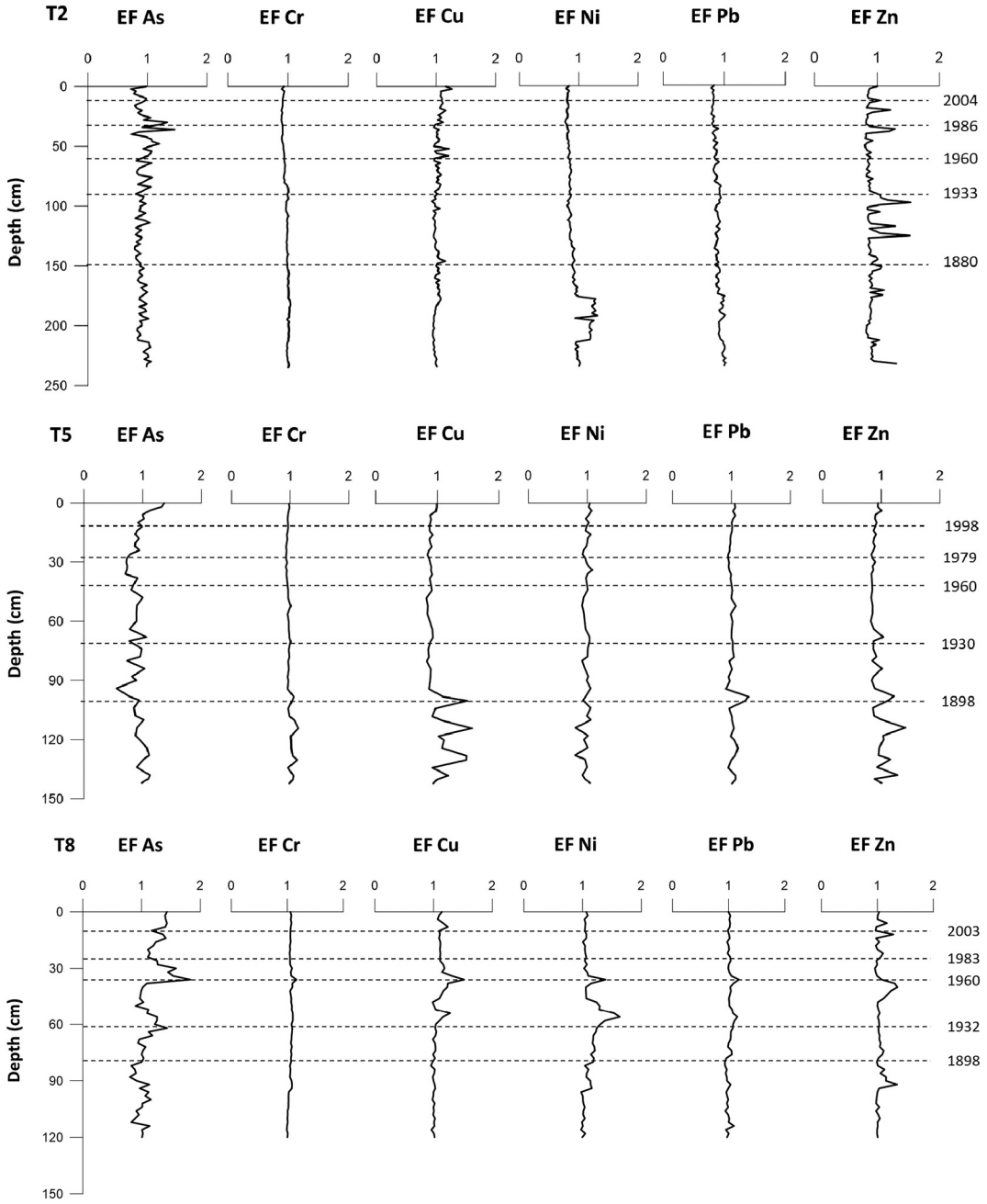

Fig. 9. Enrichment Factor (FE) of trace elements form the Caravelas sediment cores. The equivalence age-depth at some levels has been indicated through dashed lines.

Table 3
Trace elements concentrations determined in the cores analyzed in this study, in one core previously collected in the Caravelas Estuary (Sousa et al., 2014); in the Barreiras Group total concentration (Carvalho et al., 2013) together with the ERL and ERM values (Long et al., 1995).

Element (mg kg^{-1})	T2	T5	T8	Caravelas Estuary[a]	Barreiras Group	ERL	ERM
As	11.89–34.24	2.76–18.33	6.04–26.23	17.26–30.92	nd	8.2	70
Cr	24.22–45.85	8.84–42.30	9.18–36.94	49.47–62.85	25.4–59.8	81	370
Cu	3.12–6.67	1.71–5.56	1.40–4.57	4.70–7.37	3.7–13.5	34	270
Ni	5.26–12.86	1.30–9.28	1.95–7.91	11.03–15.22	7.9–18.9	20.9	51,6
Pb	6.30–23.26	3.10–11.82	2.87–11.66	11.48–17.76	9.3–22.5	46.7	218
Zn	20.81–53.29	10.98–40.16	7.89–41.88	38.66–49.16	21.8–41.0	150	410

nd: not determined.
[a] Sousa et al. (2014).

fluxes of trace elements studied (Fig. 7). According to the historical data from the Brazilian National Agency of Water (ANA, 2016) during the period of 1975–2013 (Fig. 6), the average discharge of the Peruípe river is approximately 20 $m^3 s^{-1}$ with some annual variations. An increasing trend is observed in mean discharges at the Helvécia station, from approximately 15 $m^3 s^{-1}$ in 1975 to 35 $m^3 s^{-1}$ in 1985. Following this period, there is a sharp decrease in mean discharges, reaching approximately 10 $m^3 s^{-1}$ in 1989. Another sharp increase is observed in the following years, reaching to its maximum mean discharges in 1993, followed by another sharp decrease and reaching its minimum average discharges in the late 1990s. Another increase could be seen in the early 2000s, reaching up to 30 $m^3 s^{-1}$ and, finally a decreasing trend in the following years.

Since the Caravelas estuary contributes with a small continental input and despite dominant ebb flows, the difference in suspended sediment particles at each tidal phase results in a residual transport upestuary (Schettini et al., 2013). This confirms the hypothesis of Sousa et al. (2016) that sediments originating from different areas are transported to the inner shelf by adjacent rivers (e.g., the Itanhaém and Peruípe rivers, at approximately 20 km to the north and south, respectively) and may be advected to the Caravelas estuary. Therefore, in addition to the net importation from the inner shelf, the Caravelas estuary also receives fine-grained sediment and associated trace elements inputs from the Peruípe river via the interconnection channel with the Nova Viçosa estuary.

Finally, the increasing trend of trace metal fluxes in recent years supports the idea of land use changes (Souza, 2015), that the region has been subjected to, especially due to the developments of the monoculture of eucalyptus, which has enhanced the erosion and runoff of contaminated soils from the catchment.

6. Conclusions

Based on the analysis of trace elements and their enrichment factors in the studied sediment cores studied and on the comparison with previous studies, we conclude that the Caravelas estuary has no significant contamination by Cr, Cu, Ni, Pb and Zn. Based on elemental and mineralogical analyses and their comparison with other studies on the region, the high values of As observed in the sediment cores are related to the crystalline basement of the region and to the weathering of rocks from the Barreiras Group formation. Since only slight increases in enrichment factors of As have been observed, we conclude that the enhancement of contamination in this area is due to land use changes rather than direct industrial and urban contamination sources.

The environmental changes detected in the studied sediments were essentially related to the opening of the Tomba inlet. In general, it is observed an increase in the influence of marine processes in the sediment record, since the early 1960s, with the opening of this new inlet which facilitated material exchange between the Caravelas estuary and the adjacent shelf. This opening drastically changed the hydrodynamics of the estuary, increasing the water and sediment inputs from the Nova Viçosa estuary to the Caravelas estuary.

Our results present important information that identifies modifications in the hydrodynamics and metal inputs, throughout the last decades, in an ecosystem with a great economic and ecological importance. Predictive trends for estuarine environments can be derived from the results. Such information is vital for the effective management of coastal systems, mainly when considering ongoing changes in its forcing conditions that can be exacerbated by climate change effects.

Acknowledgments

This work was funded through a FAPESP (2013/00102-8) project and CNPq scholarships (140222/2015-4 and 232299/2014-5) to JLFA, including a fellowship stay at the University of Vigo (Spain) under BR guidance. ES and RCLF are CNPq research fellows.

References

Álvarez-Iglesias, P., Rubio, B., 2012. Trace metals in shallow marine sediments from the Ría de Vigo: sources, pollution, speciation and early diagenesis. In: Panagiotaras, D. (Ed.), Earth's System Processes. INTECH Open Access Publisher, pp. 185–210.
Álvarez-Vázquez, M.A., Caetano, M., Álvarez-Iglesias, P., Pedrosa-Garcia, M.C., Calvo, S., Uña-Alvarez, E., Quintana, B., Vale, C., Prego, R., 2017. Natural and Anthropocene fluxes of trace elements in estuarine sediments of Galician Rias. Estuar. Coast. Shelf Sci. 198 (B), 329–342.
ANA (Agência Nacional de Águas), 2016. Agência Nacional de Águas. http://www.ana.gov.br.
Andrade, A.C.S., Dominguez, J.M.L., 2005. Holocene barrier Island-Lagoon system at Caravelas Strandplain, Bahia, Brazil. J. Coast. Res. 42, 164–173.
Andutta, F.P., Miranda, L.B., Schettini, C.A.F., Siegle, E., Silva, M.P., Izumi, V.M., Chagas, F.M., 2013. Temporal variations of temperature, salinity and circulation in the Peruípe river estuary (Nova, Viçosa, BA). Cont. Shelf Res. 70, 36–45.
Andutta, F.P., Helfer, F., Miranda, L.B., Deleersnijder, E., Thomas, C., Lemckert, C., 2016. An assessment of transport timescales and return coefficient in adjacent tropical estuaries. Cont. Shelf Res. 124, 49–62.
Angeli, J.L.F., Venturini, N., Ferreira, P.A.L., Figueira, R.C.L., 2016. Recent sedimentation rates in the Caravelas estuary (Bahia, Brazil) using unsupported ^{210}Pb and ^{137}Cs modeling. Radiochim. Acta 104 (7), 513–522.
Appleby, P.G., Olfield, F., 1978. The calculation of Lead-210 dates assuming a constant rate of supply of unsupported ^{210}Pb to the sediment. Catena 5, 1–8.
Barroso, C.P., 2009. Dinâmica de bancos e pontais arenosos associados à desembocadura do estuário de Caravelas, BA (Master thesis). Universidade de São Paulo (117 pp).
Birch, G.R., 2017. Determination of sediment background concentrations and enrichment in marine environments – a critical review. Sci. Total Environ. 580, 813–831.
Carvalho, S.R., Vilas Boas, G.S., Fadigas, F.S., 2013. Concentrações naturais de metais pesados em solos derivados de sedimentos do Grupo Barreiras. Cad. Geociênc. 10, 97–107.
Cochran, J.K., Hirschberg, D.J., Wang, J., Dere, C., 1998. Atmospheric deposition of metals to coastal waters (Long Island Sound, New York, USA): evidence from salt-marsh deposits. Estuar. Coast. Shelf Sci. 46, 503–522.
Dai, J., Song, J., Li, X., Yuan, H., Li, N., Zheng, G., 2007. Environmental changes reflected by sedimentary geochemistry in recent hundred years of Jiaozhou Bay, North China. Environ. Pollut. 145, 656–657.
D'Angiolella, G., Vasconcelos, V.L.D., Rosa, J.W.C., 2005. Estimativa e espacialização do balanço hídrico na meso região sul da Bahia. XII Simpósio Brasileiro de Sensoriamento Remoto (Goiânia, Goiás, Brasil). pp. 83–90.
Debenay, J.P., Duleba, W., Bonetti, C., Sousa, S.H.M., Eichler, B.B., 2001. *Paratolia cananeiaensis* n. sp.; indicator of marine influence and water circulation in Brazilian coastal and paralic environments. J. Foramin. Res. 31 (2), 152–163.
Di Leonardo, R., Cundy, A.B., Bellanca, A., Mazzola, A., Vizzini, S., 2012. Biogeochemical evaluation of historical sediment contamination in the Gulf of Palermo (NW Sicily): analysis of pseudo-trace elements and stable isotope signals. J. Mar. Syst. 94, 185–196.
Dittmar, T., Hertkorn, N., Kattner, G., Lara, R.J., 2006. Mangroves, a major source of dissolved organic carbon to the oceans. Glob. Biogeochem. Cycles 20 (102).
Dutra, L.X.C., Kikuchi, R.K.P., Leão, Z.M.A.N., 2006. Effects of sediment accumulation on reef corals from Abrolhos, Bahia, Brazil. J. Coast. Res. 39, 633–638.
Elkady, A.A., Sweet, S.T., Wade, T.L., Klein, A.G., 2015. Distribution and assessment of heavy metals in the aquatic environment of Lake Manzala, Egypt. Ecol. Indic. 58, 445–457.
Falcão, L.C., Ayres Neto, A., 2010. Parâmetros físicos de sedimentos marinhos superficiais da região costeira de Caravelas, sul da Bahia. Rev. Bras. Geof. 28 (2), 279–289.
Guo, Y., Yang, S., 2016. Heavy metal enrichments in the Changjiang (Yangtze River) catchment and on the inner shelf of the East China Sea over the last 150 years. Sci. Total Environ. 543, 105–115.
Gyllencreutz, R., Mahiques, M.M., Alves, D.V.P., Wainer, I.K.C., 2010. Mid- to late-Holocene paleoceanographic changes on the southeastern Brazilian shelf based on grain size records. The Holocene 20, 863–875.
Helali, M.A., Oueslati, W., Zaaboub, N., Added, A., Aleya, L., 2016. Bioavailability and assessment of heavy metal pollution in sediment cores off the Mejerda River Delta (Gulf of Tunis): how useful is a multiproxy approach? Mar. Pollut. Bull. 105, 215–225.
Hingston, J.A., Collins, C.D., Murphy, R.J., Lester, J.N., 2001. Leaching of chromated copper arsenate wood preservatives: a review. Environ. Pollut. 111, 53–66.
Horowitz, A.J., Elrick, K.A., 1987. The relation of stream sediment surface area, grain size and composition to trace element chemistry. Appl. Geochem. 2, 437–451.
IBGE, 2017. Censo Demográfico. Available at: http://www.ibge.gov.br (Accessed in April, 2018).
Ip, C.C.M., Li, X.-D., Zhang, G., Waia, O.W., Lia, Y.-S., 2007. Trace metal distribution in sediments of the Pearl River Estuary and the surrounding coastal area, South China. Environ. Pollut. 147, 311–323.
Lamb, A.L., Wilson, G.P., Leng, M.J., 2006. A review of coastal paleoclimate and relative sea-level reconstructions using delta C-13 and C/N ratios in organic material. Earth Sci. Rev. 75 (1–4), 29–57.
Leão, Z.M.N., Dominguez, J.M.L., 2000. Tropical coast of Brazil. Mar. Pollut. Bull. 41 (1–6), 112–122.
Leão, Z.M.A.N., Dutra, L.X.C., Spano, S., 2006. The characteristics of bottom sediments. In: Dutra, G.F., Allen, G.R., Werner, T., McKenna, S. (Eds.), The Rapid Marine Biodiversity Assessment of the Abrolhos Bank, Bahia, Brazil. RAP Bulletin of Biological Assessment, Washington, pp. 75–80.
Leipe, T., Knoppers, B., Marone, E., Camargo, R., 1999. Suspended matter transport in

coral reef waters of the Abrolhos Bank, Brazil. Geo-Mar. Lett. 19, 186–195.
Lessa, G.C., Cirano, M., 2006. On the circulation of a coastal channel within the Abrolhos Coral-Reef System – Southern Bahia (17°40′S), Brazil. J. Coast. Res. 39, 450–453.
Long, E.R., Macdonald, D.D., Smith, S.L., Calder, F.D., 1995. Incidence of adverse biological effects within ranges of chemical concentrations in marine and estuarine sediments. Environ. Manag. 19 (1), 81–97.
Loring, D.H., Rantala, R.T.T., 1992. Manual for the geochemical analyses of marine sediments and suspended particulate matter. Earth Sci. Rev. 32, 235–283.
Lubis, A.A., 2006. Constant rate of supply (CRS) model for determining the sediment accumulation rates in the coastal area using ^{210}Pb. J. Coast. Dev. 10 (1), 9–18.
Mahiques, M.M., Wainer, I.E.K.C., Burone, L., Sousa, S.H.M., Silveira, I.C.A., Bícego, M.C., Alves, D.P., Hammer, O., 2009. A high-resolution Holocene record on the Southern Brazilian shelf: paleoenvironmental implications. Quat. Int. 206, 52–61.
Martins, C.C., Bícego, M.C., Figueira, R.C.L., Angeli, J.L.F., Combi, T., Gallice, W., Mansur, A.V., Nardes, E., Rocha, M.L., Wisnieski, E., Ceschim, L.M.M., Ribeiro, A.P., 2012. Multi-molecular markers and metals as tracers of organic matter inputs and contamination status from an Environmental Protection Area in the SW Atlantic (Laranjeiras Bay, Brazil). Sci. Total Environ. 417–418.
Meyers, P.A., 1994. Preservation of elemental and isotopic source identification of sedimentary organic matter. Chem. Geol. 114, 289–302.
Meyers, P.A., 2003. Applications of organic geochemistry to paleolimnological reconstructions: a summary of examples from the Laurentian Great Lakes. Org. Geochem. 34 (2), 261–289.
Mirlean, N., Baisch, P., Travassos, M.P., Nassar, C., 2011. Calcareous algae bioclast contribution to sediment enrichment by arsenic on the Brazilian subtropical coast. Geo-Mar. Lett. 31, 65–73.
Montero, N., Belzunce-Segarra, M.J., Del Campo, A., Garmendia, J.M., Ferrer, L., Larreta, J., González, M., Maidana, M.A., Espino, M., 2013. Integrative environmental assessment of the impact of Pasaia harbour activities on the Oiartzun estuary (southeastern Bay of Biscay). J. Mar. Syst. 109–110, 252–260.
Ogrinc, N., Fontolan, G., Faganeli, J., Covelli, S., 2005. Carbon and nitrogen isotope compositions of organic matter in coastal marine sediments (the Gulf of Trieste, N Adriatic Sea): indicators of sources and preservation. Mar. Chem. 95 (3–4), 163–181.
Olbrich, B.W., Le Roux, D., Poulter, A.G., Bond, W.J., Stock, W.D., 1993. Variation in water use efficiency and δ^{13}C levels in *Eucalyptus grandis* clones. J. Hydrol. 150, 615–633.
Pereira, M.D., Siegle, E., Miranda, L.B., Schettini, C.A.F., 2010. Hidrodinâmica e transporte de material particulado em suspensão em um estuário dominado por maré: Estuário de Caravelas (BA). Rev. Bras. Geof. 28, 427–444.
Prahl, F.G., Ertel, J.R., Goni, M.A., Sparrow, M.A., Eversmeyer, B., 1994. Terrestrial organic carbon contributions to sediments on the Washington margin. Geochim. Cosmochim. Acta 58, 3035–3048.
Prajith, A., Purnachandra Rao, V., Chakraborty, P., 2016. Distribution, provenance and early diagenesis of major and trace metals in sediment cores from the Mandovi estuary, western India. Estuar. Coast. Shelf Sci. 170, 173–185.
Rao, V.P., Shynu, R., Singh, S.K., Naqvi, S.W.A., Kessarkar, P.M., 2015. Mineralogy and Sr-Nd isotopes of SPM and sediment from the Mandovi and Zuari estuaries: influence of weathering and anthropogenic contribution. Estuar. Coast. Shelf Sci. 156, 103–115.
Rubio, B., Nombela, M.A., Vilas, F., 2000. Geochemistry of major and trace elements in sediments of the Ria de Vigo (NW Spain): an assessment of metal pollution. Mar. Pollut. Bull. 40 (11), 968–980.
Sampei, Y., Matsumoto, E., 2001. C/N ratios in a sediment core from Nakaumi Lagoon, southwest Japan – usefulness as an organic source indicator. Geochem. J. 35, 189–205.
Schettini, C.A.F., Miranda, L.B., 2010. Circulation and suspended matter transport in a tidally dominated estuary: Caravelas estuary, Bahia, Brazil. Braz. J. Oceanogr. 58, 1–11.
Schettini, C.A.F., Pereira, M.D., Siegle, E., Miranda, L.B., Silva, M.P., 2013. Residual fluxes of suspended sediment in a tidally dominated tropical estuary. Cont. Shelf Res. 70, 27.
Schropp, S.J., Windom, H.L., 1988. A Guide to the Interpretation of Metal Concentrations in Estuarine Sediments. Florida Department of Environmental Regulation. Coastal Zone Management Section, pp. 44.
Siegle, E., 2016. Processos costeiros em áreas controladas por recifes: região de Abrolhos (Promotion thesis). University of São Paulo, São Paulo, Brazil (90 p).
Silva, A.S., Leão, Z.M.A.N., Kikuchi, R.K.P., Costa, A.B., Souza, J.R.B., 2013. Sedimentation in the coastal reefs of Abrolhos over the last decades. Cont. Shelf Res. 70, 159–167.
Smallwood, B., Wooller, M.J., Jacobson, M.E., Fogel, M.L., 2003. Isotopic and molecular distributions of biochemical from fresh and buried *Rhizophora mangle*. Geochem. Trans. 4 (7), 38–46.
Soares, M.L.G., Chaves, F.O., Estrada, G.C.D., Cavalcanti, V.F., Portugal, A.M.M., Barbosa, B., 2008. Caracterização das florestas de mangue do Complexo Estuarino de Caravelas (Bahia-Brasil). Bol. Téc. Cient. CEPENE 16 (5), 23–41.
Sousa, S.H.M., Amaral, P.G.C., Martins, V., Figueira, R.C.L., Siegle, E., Ferreira, P.A.L., Silva, I.S., Shinagawa, E., Salaroli, A., Schettini, C.A.F., Santa Cruz, J., Mahiques, M.M., 2014. Environmental evolution of the Caravelas Estuary (northeastern Brazilian coast, 17° S, 39° W) based on multiple proxies in a sedimentary record of the last century. J. Coast. Res. 30, 474–486.
Sousa, S.H.M., Ferreira, P.A.L., Martins, M.V.A., Siegle, E., Amaral, P.G.C., Figueira, R.C.L., Yamashita, C., Rodrigues, A.R., Mahiques, M.M., 2016. Spatial sediment variability in a tropical tide dominated estuary: sources and drivers. J. S. Am. Earth Sci. 72, 115–125.
Souza, S., 2015. Geotechnologies applied to time-space analysis of land use and occupation in coastal Plain of Caravelas (BA). Bol Goia. Geograf. 35 (1), 71–89.
Souza, J.R.B., Costa, A.B., Azevedo, A.E.G., Santos, T.H.R., Spano, S., Lentini, C.A.D., Bonabamba, T.J., Silva, R.O., Novotny, E.H., Zucchi, M.R., 2013. Carbon and nitrogen stable isotope compositions of organic matter in marine sediment cores from the Abrolhos region: indicators of sources and preservation. Geochim. Bras. 27 (1), 13–23.
Spano, S., Belem, A.L., Doria, R.N., Zucchi, M.R., Souza, J.R.B., Costa, A.B., Lentini, C.A.D., Azevedo, A.E.G., 2014. Application of organic carbon and nitrogen stable isotope and C/N ratios as source indicators of organic matter of Nova Viçosa-Caravelas estuarine complex, Southern Bahia, Brazil. Braz. J. Geol. 44 (1), 13–21.
Summerhayes, C.P., Melo, U., Barreto, H.T., 1976. The influence of upwelling on suspended matter and shelf sediments off south-eastern Brazil. J. Sediment. Petrol. 46, 818–834.
Teixeira, C. E. P, 2006. Caracterização e variabilidade da hidrodinâmica da zona costeira adjacente ao banco de Abrolhos (Master thesis). Oceanographic Institute, USP, São Paulo (93 p).
Turekian, K.K., Wedepohl, K.H., 1961. Distribution of the elements in some major units of the Earth's crust. Geol. Soc. Am. Bull. 72, 175–192.
USEPA (United States Environmental Protection Agency), 1996. Method 3050B. Acid Digestion of Sediments, Sludges and Soil. Revision 2. December.
Victor, S., Golbuu, Y., Wolanski, E., Richmond, R.H., 2004. Fine sediment trapping in two mangrove-fringed estuaries exposed to contrasting land-use intensity, Palau, Micronesia. Estuar. Coast. Shelf Sci. 12, 277–283.
Vilas Boas, G.S., Sampaio, F.J., Pereira, A.M.S., 2001. The Barreiras Group in the Northeastern coast of the State of Bahia, Brazil: depositional mechanisms and processes. An. Acad. Bras. Cienc. 73, 417–427.
Wang, J., Liu, G., Zhang, J., Liu, H., 2015. Geochemical normalization and assessment of heavy metals (Cu, Pb, Zn and Ni) in sediments from the Huaibe River, Anhui, China. Catena 129, 30–38.
Wangersky, P.J., 1986. Biological control of trace metal residence, time and speciation: a review and synthesis. Mar. Chem. 19, 269–297.
Wedepohl, K.H., 1971. Environmental influences on the chemical composition of shales and clays. In: Ahrens, L.H., Press, F., Runcorn, S.K., Urey, H.C. (Eds.), Physics and Chemistry of the Earth. Pergamon, Oxford, pp. 307–331.
Wedepohl, K.H., 1991. The composition of the upper Earth's crust and the natural cycles of selected metals: metals in natural raw materials; natural resources. In: Merian, E. (Ed.), Metals and Their Compounds in the Natural Environment. VCH, Weinheim, pp. 317.
Weis, J.S., Weis, P., 1993. Trophic transfer of contaminants from organisms living by chromated-copper-arsenate (CCA)-treated wood to their predators. J. Exp. Mar. Biol. Ecol. 168, 25–34.